HHS Public Access

Author manuscript

Biomaterials. Author manuscript; available in PMC 2018 March 01.

Published in final edited form as:

Biomaterials. 2017 March ; 121: 155–166. doi:10.1016/j.biomaterials.2017.01.003.

RhoA knockdown by cationic amphiphilic copolymer/siRhoA polyplexes enhances axonal regeneration in rat spinal cord injury model

So-Jung Gwak[1], **Christian Macks**[1], **Da Un Jeong**[1], **Mark Kindy**[2], **Michael Lynn**[3], **Ken Webb**[1], and **Jeoung Soo Lee**[1]

[1]Drug Design, Development, and Delivery (4D) Laboratory, Department of Bioengineering, Clemson University, Clemson, SC 29634

[2]Department of Pharmaceutical Sciences, College of Pharmacy, University of South Florida, Tampa, FL 33612

[3]Department of Neurosurgery, Greenville Health System, Greenville, SC 29615

Abstract

Spinal cord injury (SCI) results in permanent loss of motor and sensory function due to developmentally-related and injured-induced changes in the extrinsic microenvironment and intrinsic neuronal biochemistry that limit plasticity and axonal regeneration. Our long term goal is to develop cationic, amphiphilic copolymers (poly (lactide-co-glycolide)-g-polyethylenimine, PgP) for combinatorial delivery of therapeutic nucleic acids (TNAs) and drugs targeting these different barriers. In this study, we evaluated the ability of PgP to deliver siRNA targeting RhoA, a critical signaling pathway activated by multiple extracellular inhibitors of axonal regeneration. After generation of rat compression SCI model, PgP/siRhoA polyplexes were locally injected into the lesion site. Relative to untreated injury only, PgP/siRhoA polyplexes significantly reduced RhoA mRNA and protein expression for up to 4 weeks post-injury. Histological analysis at 4 weeks post-injury showed that RhoA knockdown was accompanied by reduced apoptosis, cavity size, and astrogliosis and increased axonal regeneration within the lesion site. These studies demonstrate that PgP is an efficient non-viral delivery carrier for therapeutic siRhoA to the injured spinal cord and may be a promising platform for the development of combinatorial TNA/drug therapy.

1. Introduction

Functional recovery following spinal cord injury (SCI) is limited by multiple developmentally-related and injury-induced mechanisms that restrict plasticity and axonal regeneration in the adult central nervous system (CNS). Damaged axons that survive the

Correspondence should be addressed to Jeoung Soo Lee (ljspia@clemson.edu): Jeoung Soo Lee, Ph.D., Clemson University, Department of Bioengineering, 301 Rhodes Research Center, Clemson, SC 29634-0905, Tel: 864-656-3212, Fax: 864-656-4466.

initial insult and secondary neuronal cell death are confronted with degenerating myelin and glial scarring. Three myelin-associated inhibitors (MAIs) have been identified (Nogo-A, myelin associated glycoprotein, and oligodendrocyte myelin glycoprotein) that bind to neuronal NgR1 and PirB receptors [1-5]. In addition, reactive astrocytes in the glial scar up-regulate expression of chondroitin sulfate proteoglycans (CSPGs) that bind to PTPsigma, leukocyte common antigen-related (LAR) phosphatase, and NgR1/NgR3 [6-8]. The signaling pathways of both classes of inhibitors as well as several axon guidance molecules converge on the activation of RhoA / Rho kinase (ROCK) [9-12] Subsequent effects on downstream targets including myosin light chain, LIM kinase/cofilin, and collapsin response mediator protein 2 interfere with cytoskeletal dynamics necessary for axonal growth [13-15]. A wide range of therapeutic strategies targeting growth inhibitory ligands, their receptors, and Rho/ROCK signaling have been shown to increase axonal regeneration and improve functional recovery, including preclinical primate models and initial human clinical trials [16-18]. However, the incomplete and variable regenerative response achieved by these approaches suggests the existence of additional barriers that restrict regeneration.

Recently, analyses of embryonic CNS neurons, the dorsal root ganglion conditioning lesion model, and transcriptomic/proteomic comparisons of PNS/CNS injury response have highlighted the importance of intrinsic neuronal biochemistry in determining regenerative capacity [19-21]. Relative to adult CNS neurons, these models have identified substantial differences in retrograde injury signaling [22], axonal transport [23], microtubule stability/organization [24], mTOR activation [25, 26], cAMP levels [27], and transcription factor expression [26, 28, 29]. One of the most promising intrinsic targets is phosphatase and tensin homolog (PTEN) that negatively regulates the Akt and mTOR pathways involved in cell survival and metabolism, respectively [30]. However, PTEN deletion alone does not elicit a maximal regenerative response and can be significantly enhanced by co-deletion of Nogo or suppressor of cytokine signaling 3 (SOCS3), a negative regulator of the Jak/STAT signaling pathway activated by some neurotrophic factors [31, 32]. Similarly, improved anatomical and functional outcomes have been achieved in several preclinical models using two or more treatments to simultaneously activate intrinsic growth capacity and neutralize extrinsic growth inhibition [33-35]. Collectively, these studies demonstrate the importance of combination therapies in overcoming the complex barriers to regeneration in the adult CNS [36-38].

Our long-term goal is to develop neuron-specific, micellar nanotherapeutics for combinatorial delivery of siRNA and hydrophobic drugs to the injured CNS. Toward this end, we have previously synthesized and characterized a cationic, amphiphilic block co-polymer, poly (lactide-co-glycolide)-graft-polyethylenimine (PgP) [39]. PgP micelles offer a hydrophobic core for solubilization of neuroprotective or neurogenic drugs, while the cationic shell can form polyelectrolyte complexes with therapeutic nucleic acids. siRNA offers several advantages for neural regeneration applications, including the large number of CNS targets therapeutically responsive to knockdown (RhoA, PTEN, SOCS3, etc.), specificity, and the ability to design sequences for different targets with minimal change in overall physicochemical properties that might affect carrier interactions and delivery properties. Previously, we have shown that PgP can efficiently transfect a variety of neural cell lines *in vitro* in the presence of 10 % serum as well as deliver pDNA to the normal rat

spinal cord [39]. Using RhoA as a well-established therapeutic target, here we investigate the ability of PgP to deliver siRNA (siRhoA) in B35 cells and in a rat compression spinal cord injury model. We show that PgP/siRhoA exhibits increased tissue retention time relative to naked siRNA after local injection and maintains RhoA knockdown for up to 4 weeks, resulting in reduced apoptosis and cavitation/astrogliosis and increased axonal regeneration relative to untreated SCI animal groups.

2. Materials and Methods

2.1. Materials

Poly (lactide-co-glycolide) (PLGA 4 kDa, 50:50) with a carboxylic end group was purchased from Durect Corporation (Pelham, AL). Branched polyethylenimine (bPEI, 25 kDa), dicyclohexylcarbodiimide (DCC), N-hydroxysuccinimide (NHS), and heparin sodium salt from porcine intestinal mucosa were purchased from Sigma-Aldrich (St. Louis, MO). Carbon-coated grid and 0.5 % Ruthenium tetroxide (RuO_4) solution were obtained from Electron Microscopy Sciences (Electron Microscopy Sciences, PA). The silencer® Pre-designed siRNA targeting RhoA (ras homolog family member A, NCBI Reference Sequence: NM_057132.3, siRhoA) and Silencer Negative Control siRNA (NT-siRNA) were purchased from Ambion (Austin, TX). RNeasy plus mini kit and QuantiTect®SYBR Green PCR Kit were purchased from Qiagen (Valencia, CA). Protein marker and a molecular weight ladder (1kb DNA Ladder) were from Bio-Rad (Hercules, CA). BCA protein assay kit, N-PER™ neuronal protein extraction reagent and albumin standard were obtained from Thermo Fisher (Rockford, IL). Label IT® siRNA Tracker Intracellular Localization Kit was purchased from Mirus (Madison, WI) and ApopTag® Plus In Situ Apoptosis Fluorescein Detection Kit from EMD Millipore (Billerica, MA). Dulbecco's Modification of Eagle's Medium/Ham's F-12 50/50 mix with L-glutamine (DMEM/F12), 100× stock solution of penicillin/streptomycin, and 0.05 % trypsin/0.53 mM EDTA in Hank's Balanced Salt Solution were obtained from Mediatech Inc (Manassas, VA) and fetal bovine serum (FBS) from Hyclone (Logan, UT). Other reagents were commercial special-grade, used without further purification.

2.2. Stability of PgP/siRNA polyplexes by gel retardation assay

Cationic, amphiphilic copolymer PgP (poly(lactide-co-glycolide)–g-polyethylenimine) was synthesized using PLGA (4 kDa, 50:50) with a carboxylic end group and branched polyethylenimine (bPEI, 25 kDa) as previously described [39]. The formation of stable polyplexes was evaluated by gel retardation assay. PgP/siRhoA polyplexes were prepared at various N/P ratios in deionized water and incubated for 30 minutes at 37 °C. bPEI/siRhoA polyplexes at N/P ratio 5/1 and RNAiMAX/siRhoA prepared according to the manufacturer's instructions were included as controls. The polyplexes were loaded on a 2 % (w/v) agarose gel and electrophoresed for 90 minutes at 80 V. The gel was stained with ethidium bromide (0.5 μg/ml) for 30 minutes and imaged on a UV illuminator (Alpha Innotech FluorChem SP imager) to visualize the migration of polyplexes and naked siRhoA.

2.3. Knockdown efficiency and cytotoxicity of PgP/siRhoA polyplexes in serum condition *in vitro*

B35 neuroblastoma cells (CRL-2754, ATCC, Manassas, VA) were seeded in 24-well plates at a density of 8×10^4 cells/well in 10 % serum-supplemented medium. After overnight incubation, the cells were washed twice with fresh medium. PgP/siRhoA polyplexes (1μg of siRhoA) at N/P ratios ranging from 5/1 to 30/1 were prepared. PgP/NT-siRNA at N/P ratio of 30/1, bPEI/siRhoA polyplex at N/P ratio of 5/1, and RNAiMAX/siRhoA prepared according to manufacturer's protocol were also included for comparison. Non-transfected cells were used as a control. The cells were transfected with polyplexes in medium containing 10 % FBS, incubated for 24 hours and then the media containing polyplexes were removed and replaced by fresh medium containing 10 % FBS. The cells were incubated an additional 48 hours. At 72 hours post-transfection, the cells were lysed and total RNA was isolated using RNeasy mini kit. The isolated RNA quality and quantity were evaluated by Take 3 using a BioTek synergy microplate reader (BioTek, Synergy HT). Complementary DNA (cDNA) was synthesized by reverse transcription reactions with isolated total RNA (0.5 μg) using moloney murine leukemia virus (MMLV) reverse transcriptase with oligo (dT) primers (RetroScript Kit; Ambion). Real-time PCR was performed using target-specific primers (final concentration: 0.5 μM) using SYBR Green PCR kit in a Rotorgene Q thermal cycler (Qiagen). Glyceraldehyde-3-phosphate dehydrogenase (GAPDH) was used as an endogenous control. Primers for Rho A: forward primer: 5′-TTC GGA GTC GTC GTC TTG AG-3′, reverse primer: 5′-CCA CAA GCT CCA TCA CCA AC -3′. Primers for GAPDH: forward primer: 5′- ATG GCC TTC CGT GTT CCT AC-3′; reverse primer: 5′-AAC TTT GGC ATC GTG GAA GG -3′. The cycle number at which the amplification plot crosses the threshold was calculated (CT). Relative mRNA expression levels of RhoA were calculated using the $2^{-\Delta\Delta}$ Ct method [40]. The minus RT (reverse transcriptase) reactions performed on a representative subset of samples demonstrated that genomic DNA contamination was not significant (data not shown). Reaction specificities were routinely verified by melting curve analysis.

Cytotoxicity of polyplexes in B35 cells was analyzed by MTT assay in parallel experiments. At 72 hours post-transfection, media were replaced with fresh DMEM/F12 without serum and 250 μl of thiazolyl blue tetrazolium bromide (MTT, Sigma-Aldrich) solution in PBS (2 mg/ml) was added to each well. Plates were incubated for 4 hours at 37 °C and then washed with PBS. The formazan crystals formed by live cells were dissolved in DMSO and absorbance was measured at 570 nm. Cell viability (%) was calculated relative to non-transfected control according to the following equation:

$$\text{Cell viability}(\%) = (\text{OD}_{570(\text{sample})} / \text{OD}_{570(\text{control})}) \times 100\%$$

2.4. Characterization and stability of PgP/siRhoA polyplexes

2.4.1. Particle size, ζ-potential, and morphology of PgP/siRhoA polyplexes—

PgP/siRhoA polyplexes at N/P ratio 30/1 were prepared by adding 500 μl (20 μg) of siRhoA in nuclease-free water into 500 μl of PgP in nuclease-free water, followed by gentle mixing

and incubation for 30 minutes at 37 °C. Poly plex particle size was measured by dynamic laser light scattering (DLS) and ζ-potential (ZP) was measured electrophoretically using Zeta PALS (Brookhaven Instruments Corp, Holtsville, NY).

The morphology of PgP/siRhoA polyplex at N/P ratio of 30/1 was imaged by transmission electron microscopy (TEM, Hitachi H-7600, Tokyo, Japan). Five μl of polyplex solution were placed onto a carbon coated copper grid and dried at room temperature. The specimens were vapor-stained with 0.5 % Ruthenium tetroxide (RuO_4) solution to improve the contrast and imaged by TEM at an acceleration voltage of 100 kV and magnifications of ×200×.

2.4.2. Stability of PgP/siRNA polyplexes in the presence of serum—To evaluate the stability of PgP/siRhoA polyplexes in the presence of serum, polyplexes prepared at N/P ratio of 30/1 were incubated in medium containing 10 % serum at 37 °C. At pre-determined time points, polyplexes were evaluated by 2 % (w/v) agarose gel electrophoresis.

2.4.3. Stability of PgP/siRNA polyplexes by heparin competition assay—The stability of PgP/siRhoA polyplexes was also evaluated by heparin competition assay. Briefly, PgP/siRhoA at N/P ratio 30/1 was incubated with heparin solution at 0-40 heparin/siRNA w/w ratio at 37 °C for 30 minutes. Th e samples were immediately analyzed by 2 % (w/v) agarose gel electrophoresis. bPEI/siRhoA at N/P ratio of 5/1 was used for comparison.

2.4.4. Shelf-life of PgP/siRNA polyplexes—To evaluate stability during storage, PgP/siRhoA polyplexes at N/P ratio of 30/1 were stored at 4 °C for 4 weeks. At 1, 2, 3, and 4 week time points, polyplexes were sampled and analyzed by agarose gel electrophoresis. To confirm siRNA integrity after storage, 4 week samples dissociated with heparin (10 w/w heparin/siRNA ratio) at 37 °C for 30 minutes were also evaluated.

2.5. Generation of rat compression spinal cord injury model

All surgical procedures and postoperative care were conducted according to NIH guidelines for the care and use of laboratory animal (NIH publication No. 86-23, revised 1996) and under the supervision of the Clemson University Animal Research Committee (Approved animal protocol no. AUP2014-012). The compression SCI was performed as previously described by Gwak et al [41]. Briefly, Sprague Dawley rats (male, 200 gm, Charles River) were deeply anesthetized with isoflurane gas. Their backs were shaved and prepared with betadine solution, chlorhexidine, and sterile water. The T9 spinous processes were identified and a 4-cm longitudinal incision over the dorsal mid-thoracic region was made using a #10-blade scalpel. The T9 spinous processes were removed using orthopedic bone cutter and rongeurs and the ligamentum flavum was removed to expose the intervertebral space. A vascular clip was inserted through the dorsal T8~T9 intervertebral space and the spinal cord was compressed for 10 minutes. Following injury, the paraspinal muscles were closed with 4–0 vicryl suture and the skin was closed with 3-0 silk suture. After surgery, animals were warmed by heating blanket for recovery. For 2 weeks after surgery, animals received antibiotics cefazolin (40 mg/Kg, Hikma Farmaceutic) and analgesic buprenorphine (0.01 mg/kg, Hospira Inc) and bladders were manually expressed three times daily.

2.6. Retention and cellular uptake of polyplexes in SCI lesion after local injection

The retention of polyplexes after local injection into SCI lesion site was evaluated using Cy5 conjugated siRNA (siRNA-Cy5). Rat compression SCI model was generated as described above and 10 μl of PgP/siRNA-Cy5 (N/P ratio of 30/1, 10 μg siRNA-Cy5) were prepared and injected using a 26G Hamilton syringe (HAMILTON®, Reno, NV, USA) at the lesion site. Naked siRNA-Cy5 (10 μg siRNA-Cy5 in 10 μl) was used for comparison. At 6 and 24 hours post-injection, spinal cords (0.5 cm-long piece from the center of the injury) were harvested and imaged by live animal fluorescence imaging system (IVIS Luminar XR, Caliper Life Sciences).

To visualize the uptake of PgP/siRNA-Cy5 polyplexes in neuronal cells, the retrieved spinal cords were fixed with 4 % paraformaldehyde solution (pH 7.4; Merck, Kenilworth, NJ), sectioned longitudinally at 10 μm thickness, and mounted on positively charged glass slides. Sections were stained using chick anti-rat neurofilament monoclonal antibody (NF; Abcam, Cambridge, MA) followed by Alexa Fluor® 488 conjugated anti-chick IgG (Jackson ImmunoResearch Laboratories, Inc., West Baltimore Pike, PA, USA). The stained sections were digitally imaged using an inverted epifluorescent microscope (Zeiss Axiovert 200, Göttingen, Germany).

2.7. RhoA knockdown efficiency of PgP/siRhoA polyplex in SCI lesion after local injection

To optimize the N/P ratio of PgP/siRhoA polyplexes for RhoA knockdown in rat SCI model, PgP/siRhoA polyplexes were prepared at two different N/P ratios (15/1 and 30/1) using 10 μg of siRhoA and injected into the injured dorsal T9 SCI lesions. PgP/NT-siRNA at an N/P ratio of 30/1 (10 μg NT-siRNA), untreated SCI animal group, and sham animal group were used as controls. At 1 week post-injection, animals were sacrificed for RT-PCR, western blot, and immunohistochemistry (IHC).

For RT-PCR, rats (N=5/group) were sacrificed by CO_2 overdose and spinal cords (0.5 cm-long piece from the center of the injury) were retrieved. Total RNA was purified using RNeasy mini kit. RNA quality/quantity was measured and two-step real-time PCR was performed with target-specific primers performed as described above (section 2.3.).

For western blot, rats (N=3/group) were sacrificed by CO_2 overdose and spinal cords were retrieved. The samples were homogenized in N-PER™ neuronal protein extraction reagent and the total protein was measured using the BCA protein assay reagent kit. Protein samples (50 μg/lane) were electrophoresed in 10 % sodium dodecyl sulfate-polyacrylamide gel and transferred onto polyvinylidene fluoride (PVDF) membranes. The membranes were incubated with blocking buffer (5 % non-fat dry milk in phosphate buffered saline containing 0.1 % Triton X-100 (PBST)) for 1 hour at room temperature and incubated with the rabbit anti-RhoA monoclonal antibody (Thermo Fisher Scientific) and mouse anti-β-actin (Santa Cruz Biotechnology, Dallas, TX) overnight at 4°C. The me mbranes were washed and incubated with goat anti-rabbit-HRP (1:2000, Southern Biotech, Birmingham, AL) and goat anti-mouse-HRP (1:5000, Southern Biotech) for two hours at room temperature. The blots were developed using a Supersignal™ West Pico Chemiluminescent Substrate (Thermo Fisher Scientific) and ChemiDoc-IT^2 imager (UVP, Upland, CA).

For IHC, rats (N=5/group) were anesthetized by isoflurane gas and sacrificed via cardiac perfusion with 4 % paraformaldehyde solution. The retrieved spinal cords were embedded into Tissue-Tek® O.C.T compound (Sakura Finetek USA Inc, CA) on liquid nitrogen and 10 μm thick sections cut longitudinally and mouted on positively charged glass slides. The sections were stained using rabbit monoclonal anti-RhoA followed by Cy3-conjugated anti-rabbit IgG. To evaluate RhoA expression in neurons in the lesion site, sections were double immunostained using rabbit monoclonal anti-RhoA and mouse monoclonal anti-beta III tublin (2G10, Abcam) followed by Cy3-conjugated anti-rabbit IgG and Alexa Fluor® 488-conjugated anti-mouse IgG (Jackson ImmunoResearch Laboratories, Inc), respectively.

2.8. Effect of RhoA knockdown by PgP/siRhoA polyplex on apoptosis in SCI lesion after local injection

To evaluate the effect of RhoA knockdown by PgP/siRhoA polyplex at N/P ratio of 30/1 (10 μg siRhoA) on apoptosis in SCI lesion site, TUNEL assay was performed at 1 week post-injury. PgP/NT-siRNA at an N/P ratio of 30/1 (10 μg NT-siRNA) and untreated SCI animal group were used for comparison. The sections were stained by using the ApopTag Plus Fluorescein In situ Apoptosis Detection kit (Chemicon International. Temecula, CA) and nuclei were counterstained by DAPI. To identify apoptotic neurons, sections were double immunostained by both TUNEL staining and beta III tublin staining. After imaging, the number of total TUNEL positive (+) and beta-III tubulin positive (+) cells were counted using ImageJ software program.

2.9. Effect of PgP/siRhoA dosage on RhoA knockdown and axon regeneration after SCI

To evaluate the effect of dose and dosage of polyplex injection on RhoA knockdown and axon regeneration, SCI rats were divided into 4 groups as follows; 1) Single injection group: PgP/siRhoA polyplex (20 μl, N/P 30/1, siRNA 20 μg) was injected in the injury site after SCI injury, 2) Repeat injection: PgP/siRhoA polyplex (10 μl, N/P 30/1, siRNA 10 μg) was injected after SCI injury and repeated at one week post-injury, 3) untreated SCI animal group, and 4) sham animal group. The animals were sacrificed for RT-PCR at 1, 2, and 4 weeks post-injury (N=5/group) and for histological analysis at 4 weeks post-injury (N=5/group).

To measure RhoA mRNA expression, euthanasia, tissue retrieval, and RT-PCR analysis was performed as described above (section 2.3.). For histological analysis, rats were euthanized at 4 weeks post-injury and spinal cords retrieved, embedded, and sectioned longitudinally at 10 μm thickness. RhoA knockdown in the lesion site and surrounding tissue was visualized by IHC staining using anti-RhoA as described above (section 2.7). Other sections were stained with hematoxylin and eosin, imaged, and quantitative measurements of total necrotic cavity area performed in ImageJ. To evaluate the effect of RhoA knockdown on astrogliosis and axonal regeneration, sections were stained using antibodies against neurofilament for neurons (NF; Abcam) and glial fibrillary acidic protein (GFAP, Abcam) for astrocytes followed by Cy3-conjugated anti-rabbit IgG and Alexa Fluor® 488-conjugated anti-mouse IgG secondary antibody, respectively. Total 15 sections from each group (3 sections/rat, 5 rats/group) were randomly selected, digitally imaged, and the % neurofilament positive area

in the lesion site was calculated and expressed as a percentage of the total necrotic cavity area measured from hematoxylin and eosin staining.

2.10. Statistical analysis

Quantitative data are presented as the mean ± standard deviation. Statistical analysis was performed by one-way ANOVA with the Least Significant Difference (LSD) method used for *post-hoc* comparisons between subgroups. A *p*-value less than 0.05 was considered significant.

3. Results

3.1. Stability of PgP/siRNA polyplexes by gel retardation assay

To determine the optimal N/P ratio for stable PgP/siRhoA polyplex formation, a gel retardation assay was performed. Complete gel retardation was observed for PgP/siRhoA polyplexes formed at N/P ratio of 10 or above (Fig 1). This result is consistent with the stability of PgP/pDNA polyplexes observed in our previous study [39].

3.2. Knockdown efficiency and cytotoxicity of PgP/siRhoA polyplexes in serum condition *in vitro*

PgP/siRhoA polyplexes at various N/P ratios were prepared and transfected in B35 cells in media containing 10 % serum. Knockdown efficiency of PgP/siRhoA polyplexes increased with increasing N/P ratio and was significantly higher than that of bPEI (~6.7 %) at all N/P ratios (Fig. 2A). The relative silencing efficiency of PgP/siRhoA at N/P ratio of 30/1 was approximately 42 % and was less efficient than that of RNAiMAX/siRhoA (~62 %). However, viability of cells transfected with RNAiMAX/siRhoA was significantly lower than the non-transfected control, while viability of cells transfected with PgP/siRhoA polyplexes at all N/P ratios was not significantly different (Fig. 2B).

3.3. Characterization and stability of PgP/siRhoA polyplexes

3.3.1. Particle size, ζ-potential, and morphology of PgP/siRhoA polyplexes— Particle size and zeta potential of PgP/siRNA polyplexes at N/P 30/1 were evaluated in preparation for *in vivo* study. The mean size of PgP/siRNA polyplexes at N/P ratio of 30/1 was 179 ± 13.94 nm with polydispersity 0.318 ± 0.03 (sFig 1A). PgP completely neutralized the negatively charged siRNA and the average zeta potential of PgP/siRhoA polyplexes at N/P ratio of 30/1 was 48.52 ± 0.35 mV (sFig 1B). TEM imaging of PgP/siRNA polyplex at N/P ratio 30/1 showed discrete spheres with smooth surface morphology without aggregation (sFig. 1C).

3.3.2. Stability of PgP/siRNA polyplexes in the presence of serum—The stability of PgP/siRhoA polyplexes (N/P 30/1) in serum was evaluated after incubating polyplexes at 37 °C and gel electrophore sis analysis showed that PgP/siRhoA polyplexes were stable in the presence of serum up to 7 days (sFig. 2A), while naked siRNA was undetectable after 30 minutes (data not shown).

3.3.3. Stability of PgP/siRNA polyplexes by heparin competition assay—The stability of PgP/siRhoA polyplexes was also evaluated by heparin competition assay. PgP/siRhoA polyplexes (N/P ratio of 30/1) were stable in the presence of up to 2 and dissociated at 6 w/w heparin/siRNA ratio, while bPEI/siRhoA polyplexes (N/P ratio of 5/1) were dissociated and released siRNA in the presence of 0.6 w/w heparin/siRNA (sFig. 2B).

3.3.4. Shelf-life of PgP/siRNA polyplexes—To evaluate the long-term shelf stability of PgP/siRhoA polyplexes, PgP/siRNA (N/P 30/1) were stored at 4 °C. Gel electrophoresis anal ysis showed that PgP/siRNA polyplexes were stable up to 4 weeks and intact siRNA could be recovered after 4 weeks by heparin treatment (sFig. 2C).

3.4. Retention and cellular uptake of PgP/siRNA-Cy5 polyplexes after local injection in SCI lesion

Cy-5 conjugated siRNA (siRNA-Cy5) was used to compare the retention of naked siRNA and polyplexes after injection in SCI lesion sites and to confirm polyplex uptake by neuronal cells. Both naked siRNA-Cy5 and PgP/siRNA-Cy5 were detected in the lesion site and surrounding spinal cord tissue at 6 hours post-injection and the amount (fluorescence intensity) of PgP/siRNA-Cy5 was substantially higher (Fig. 3A). At the 24 hour time point, PgP/siRNA-Cy5 was still retained at the injection site and surrounding tissue, while naked siRNA-Cy5 was no longer detectable. IHC staining of spinal cord sections showed that PgP/siRNA-Cy5 polyplexes (Red) were co-localized with neurofilament positive cells (Green), confirming neuronal uptake of PgP/siRNA-Cy5 (Fig. 3B).

3.5. RhoA knockdown after local injection of PgP/siRhoA in spinal cord injury lesion

To evaluate the effect of polyplex N/P ratio, RhoA knockdown was evaluated one week after SCI and injection of PgP/siRhoA polyplexes prepared at N/P ratios of 15/1 and 30/1. RT-PCR showed that RhoA mRNA expression was significantly increased in the untreated SCI and PgP/NT-siRNA treated animal groups relative to the sham animal group (Fig 4A). In contrast, RhoA mRNA expression in animal groups treated with PgP/siRhoA polyplexes at either N/P ratio was not significantly different relative to the sham control and significantly reduced relative to untreated SCI and NT-siRNA treated animal groups. RhoA knockdown was also confirmed by western blot and RhoA expression in groups treated with PgP/siRhoA polyplexes at both N/P ratios was lower than that in untreated SCI and PgP/NT-siRNA treated animal groups. In contrast to the mRNA analysis, RhoA expression at the protein level was substantially lower in the animal group receiving PgP/siRhoA polyplexes at N/P ratio of 30/1 relative to the group receiving polyplexes prepared at N/P ratio of 15/1. (Fig 4B).

Figure 5A shows representative IHC imaging of RhoA expression in spinal cords from various animal groups. In untreated SCI animals, RhoA expression was highly upregulated relative to the sham control, while RhoA expression was not substantially increased in animals receiving PgP/siRhoA polyplex at N/P ratio of 30/1. RhoA expression was also upregulated in PgP/NT-siRNA treated animal group, confirming that the low level of RhoA expression in the experimental group was attributable to sequence-specific knockdown.

Figure 5B shows double IHC staining of RhoA and beta-III tubulin expression. Far fewer RhoA +/ beta-III-tubulin + cells were observed in animals receiving injections of PgP/siRhoA polyplexes than in both PgP/NT-siRNA polyplex and untreated SCI animal groups.

3.6. Effect of RhoA knockdown by PgP/siRhoA polyplexes on apoptosis in SCI lesions

We also evaluated the effect of RhoA knockdown on apoptosis by TUNEL assay at 1 week post-injury. Figure 6A shows representative images of total apoptotic cells (TUNEL+) in the spinal cord from various animal groups. The % TUNEL+ cells was significantly lower in animals receiving PgP/siRhoA polyplexes than both PgP/NT-siRNA and untreated SCI animal groups (Fig 6C). Figure 6B shows representative images of the beta-III+ and TUNEL + cells. The % of beta-III+/TUNEL+ cells was significantly lower in the PgP/siRhoA group than in both PgP/NT-siRNA and untreated SCI animal groups (Fig 6D).

3.7. Effect of PgP/siRhoA dosage on RhoA knockdown and axon regeneration after SCI

We next evaluated RhoA knockdown and axonal regeneration over a 4 week time period and compared the efficacy of delivering PgP/siRhoA (N/P: 30/1) as a single one-time 20 μg siRhoA dose injected immediately or as two 10 μg siRhoA doses injected immediately and at one week post-injury (Fig 7A). Figure 7B shows the relative RhoA mRNA levels in various animal groups at 1, 2, and 4 weeks post-injury. In untreated SCI animal group, the relative RhoA mRNA level was significantly higher than that in sham animal group at all time points. The relative RhoA mRNA level in both treatment groups (single injection and repeat injection) was significantly lower than that in untreated SCI animal group and reduced to levels approximately equal to those observed in sham animal group.

RhoA knockdown was also observed by IHC in spinal cord harvested from various animal groups. Figure 7C shows representative IHC imaging of RhoA in spinal cords harvested at 4 weeks post-injury. In untreated SCI animals, RhoA expression was highly upregulated, while RhoA expression in both treatment groups (single injection and repeat injection) was significantly lower relative to untreated SCI animal group.

The effect of RhoA knockdown by both treatment groups (single injection and repeat injection) on astrogliosis and axon regeneration was evaluated by double IHC staining of GFAP and neurofilament at 4 weeks post-injury (Fig 8A). In untreated SCI animal group, an extensive necrotic lesion cavity was formed and substantial reactive astrogliosis was observed in the surrounding tissue (Top). In animals receiving both single and repeated injections of PgP/siRhoA polyplexes, cavitation and astrogliosis were substantially reduced compared to untreated SCI group and axonal regeneration was observed into the lesion site (middle: single injection, bottom: repeated injection). In both single and repeat injection groups, cavity area was significantly smaller (Fig. 8B) and % neurofilament-positive area (Fig. 8C) was significantly higher than that in untreated SCI animal group. Interestingly, although RhoA knockdown was similar for both single and repeat injection, delivery of the same total dose of PgP/siRhoA polyplexes via repeated injection was much more effective at reducing cavitation, stimulating axonal regeneration, and sparing neuronal cells relative to a single injection.

Discussion

Among the wide range of extrinsic and intrinsic mechanisms that limit plasticity and axonal regeneration in the adult CNS, a large number involve constitutive or injury-induced expression of specific molecules (MAIs, CSPGs, RhoA, PTEN, SOCS3, etc.) that offer therapeutic targets for pharmacological inhibition/antagonism. Post-transcriptional gene knockdown by RNA interference is a highly specific and efficient approach to lower the expression levels of these targets and enhance regenerative capacity. As with all nucleic acid-based therapeutics, the key challenge is to overcome extracellular and intracellular barriers to delivery.

A large number of studies have successfully used virally-delivered shRNA in SCI models [42-45]. Despite their high transfection efficiency, immunogenicity and adverse effects of viral vectors in clinical trials create a compelling need for improved non-viral delivery systems.[46, 47]. A wide range of cationic lipids and polymers, including PEI, polyamidoamine (PAMAM) dendrimers, and poly (β-amino esters) have been evaluated for nonviral delivery of pDNA and small RNA therapeutics [48-50]. Currently, only a few studies have investigated non-viral delivery of siRNA in spinal cord injury models [51-53], non-viral delivery of siRNA in spinal cord injury models [51-53]. Previously, we have reported the synthesis of PgP, a micelle forming block copolymer designed for combinatorial drug/nucleic acid delivery and demonstrated its capability for *in vitro* transfection of siRNA and pDNA in the presence of serum and pDNA in the uninjured rat spinal cord [39]. Here, we investigated the ability of PgP to deliver siRNA targeting RhoA in a rat spinal cord compression injury model.

We first evaluated the stability, knockdown efficiency, and cytotoxicity of PgP/siRhoA as a function of N/P ratio *in vitro*. The knockdown efficiency of PgP/siRhoA polyplexes increased with increasing N/P ratio and appeared to reach a maximum efficiency at 20/1 and 30/1. Even though knockdown efficiency using RNAiMAX was higher than using PgP, RNAiMAX/siRhoA showed significant cytotoxicity compared to untreated control, while PgP/siRhoA did not show significant toxicity. Based on its efficacy and cytocompatibility in these and our previous studies [39], we more carefully evaluated the physico-chemical properties and stability of PgP/siRhoA polyplex at N/P ratio of 30/1. PgP/siRhoA polyplexes exhibited sub-200 nm particle size and positive charge suitable for cellular uptake by endocytosis [54]. This polyplex composition was able to provide increased protection from serum nucleases and stability in the presence of a competing anionic macromolecule (heparin) relative to bPEI, one of the most widely used nonviral vectors. In addition, PgP/siRhoA could be stably stored for up to 1 month at 4 °C, an important feature for commercial and clinical application.

A critical feature of all gene delivery systems is the choice of delivery route and residence time at the delivery site. In these studies, we used local injection to directly deliver the polyplexes to the spinal cord lesion site. PgP/siRNA-Cy5 polyplexes were retained at the injury site up to 24 hours post-injection, while naked siRNA-Cy5 was undetectable after 6 hours, likely either as a result of degradation or diffusion away from injection site. IHC analysis also demonstrated co-localization of the PgP/siRhoA-Cy5 with neurons. To our

knowledge, this is the first study to show that polyplexes exhibit increased residence time after local injection into spinal cord lesion site relative to naked siRNA. Several studies have used intrathecal injection and Otsuku et al reported preferential uptake of chemically-modified siRNA at the injury site, presumably due to increased penetration in injured tissue [51] [55]. In the future, we will investigate the delivery of PgP/siRhoA polyplexes to the injured spinal cord by the intrathecal route.

We next examined the *in vivo* efficacy of PgP/siRhoA using a fixed dose (10 μg siRhoA) and two different N/P ratios (15/1 and 30/1). A one-week time point was chosen based upon previous studies demonstrating that this corresponded to peak induction/activation of RhoA after SCI [56-58]. The effect of SCI on RhoA has varied among these studies, with some observing significant increases in mRNA/protein expression and others reporting significant increases in activated RhoA without changes in total expression levels. In the present study, we observed significant induction of RhoA mRNA expression that was effectively inhibited by PgP/siRhoA delivery. Although mRNA expression was modestly lower using PgP/siRhoA at N/P ratio of 30/1 than 15/1, increased knockdown at 30/1 was more apparent at the protein level and the efficacy of this composition was confirmed by western blot and histological analysis.

In addition to its inhibitory effects on axonal regeneration, RhoA also plays an important role in apoptosis by activating PTEN that subsequently inhibits activation of Akt and its downstream signaling cascade that promotes cell survival [59, 60]. Several studies have shown that inhibitors of Rho and ROCK prevent apoptosis and secondary neuronal and glial cell death in spinal cord and retinal injury models [7, 57, 61, 62]. Consistent with these previous observations, our TUNEL assay demonstrated that knockdown by PgP/siRhoA polyplexes significantly reduced both total and neuronal cell apoptosis.

After demonstrating successful knockdown by PgP/siRhoA polyplexes at 7 days post-injury, we next compared the effect of a fixed dose (20 μg) administered via single or repeated injection on RhoA knockdown over a 4 week time course on cavity formation, astrogliosis, and axonal regeneration. Even though we observed efficient RhoA knockdown with PgP/siRhoA polyplexes using 10 μg siRhoA at 1 weeks post-injection, we were not sure that 10 μg siRNA can achieve long-term knockdown and axon regeneration. In small drug and protein delivery, drugs are often repeatedly taken or injected to maintain the therapeutic dose and improve the long-term efficacy. For example, Bertrand *et. al.* found that repeated injections of a cell-permeable C3-like RhoA-antagonist significantly increased retinal ganglion cell survival in an optic nerve injury model [63]. Therefore, we expected that the repeated injection might maintain the drug at a therapeutic dose for a prolonged period of time and achieve improved efficacy. Although both single and repeated administration significantly reduced RhoA mRNA and protein expression up to 4 weeks, we observed that animals treated with repeated injection showed substantially reduced astrogliosis, necrotic cavity formation, and improved axonal regeneration relative to those receiving the polyplexes through a single administration. One limitation is that our present studies do not reveal why repeated administration appears to achieve superior anatomical outcomes despite similar efficacy in RhoA knockdown.

Conclusion

In this study, we demonstrate that the cationic, amphiphilic copolymer PgP can efficiently deliver siRhoA to a rat SCI lesion site and knockdown RhoA expression for up to 4 weeks. RhoA knockdown by PgP/siRhoA reduces apoptosis, cavitation, and astrogliosis and increases axonal regeneration. These results demonstrate that PgP may be a promising platform for the development of combinatorial siRNA/drug therapy. In future studies, we will further evaluate the effect of siRhoA dose, post-injury administration timing, and injection route of PgP/siRhoA polyplexes on axonal regeneration and functional recovery after SCI.

Supplementary Material

Refer to Web version on PubMed Central for supplementary material.

Acknowledgments

We thank Dr. John Parrish and Godley-Snell animal facility staff, especially Tina Parker and Travis Pruitt for their assistance for animal study. We also thank Dr. Terri Bruce from COBRE Bioengineering and Bioimaging Core and CLIF center for her technical support and access to the AZ100 microscope. Research reported in this publication was supported by NIGMS of the National Institutes of Health under award number 5P20GM103444-07 and South Carolina Spinal Cord Injury Research Foundation under award number SCIRF # 2014 I-02. Dr. Kindy is a BLR&D Senior Research Career Scientist and supported by AHA Award under # 1I01-RX001450-01A1 and VA Merit Award under #15SFDRN25710468.

References

1. Fournier AE, GrandPre T, Strittmatter SM. Identification of a receptor mediating Nogo-66 inhibition of axonal regeneration. Nature. 2001; 409:341–6. [PubMed: 11201742]
2. Chen MS, Huber AB, van der Haar ME, Frank M, Schnell L, Spillmann AA, et al. Nogo-A is a myelin-associated neurite outgrowth inhibitor and an antigen for monoclonal antibody IN-1. Nature. 2000; 403:434–9. [PubMed: 10667796]
3. Wang KC, Koprivica V, Kim JA, Sivasankaran R, Guo Y, Neve RL, et al. Oligodendrocyte-myelin glycoprotein is a Nogo receptor ligand that inhibits neurite outgrowth. Nature. 2002; 417:941–4. [PubMed: 12068310]
4. Liu BP, Fournier A, GrandPre T, Strittmatter SM. Myelin-associated glycoprotein as a functional ligand for the Nogo-66 receptor. Science. 2002; 297:1190–3. [PubMed: 12089450]
5. Atwal JK, Pinkston-Gosse J, Syken J, Stawicki S, Wu Y, Shatz C, et al. PirB is a Functional Receptor for Myelin Inhibitors of Axonal Regeneration. Science. 2008; 322:967–70. [PubMed: 18988857]
6. Shen Y, Tenney AP, Busch SA, Horn KP, Cuascut FX, Liu K, et al. PTPsigma is a receptor for chondroitin sulfate proteoglycan, an inhibitor of neural regeneration. Science. 2009; 326:592–6. [PubMed: 19833921]
7. Fisher D, Xing B, Dill J, Li H, Hoang HH, Zhao ZZ, et al. Leukocyte Common Antigen-Related Phosphatase Is a Functional Receptor for Chondroitin Sulfate Proteoglycan Axon Growth Inhibitors. J Neurosci. 2011; 31:14051–66. [PubMed: 21976490]
8. Dickendesher TL, Baldwin KT, Mironova YA, Koriyama Y, Raiker SJ, Askew KL, et al. NgR1 and NgR3 are receptors for chondroitin sulfate proteoglycans. Nature neuroscience. 2012; 15:703–12. [PubMed: 22406547]
9. Wahl S, Barth H, Ciossek T, Aktories K, Mueller BK. Ephrin-A5 induces collapse of growth cones by activating Rho and Rho kinase. The Journal of cell biology. 2000; 149:263–70. [PubMed: 10769020]

10. Fournier AE, Takizawa BT, Strittmatter SM. Rho kinase inhibition enhances axonal regeneration in the injured CNS. J Neurosci. 2003; 23:1416–23. [PubMed: 12598630]
11. Monnier PP, Sierra A, Schwab JM, Henke-Fahle S, Mueller BK. The Rho/ROCK pathway mediates neurite growth-inhibitory activity associated with the chondroitin sulfate proteoglycans of the CNS glial scar. Molecular and cellular neurosciences. 2003; 22:319–30. [PubMed: 12691734]
12. Hata K, Fujitani M, Yasuda Y, Doya H, Saito T, Yamagishi S, et al. RGMa inhibition promotes axonal growth and recovery after spinal cord injury. The Journal of cell biology. 2006; 173:47–58. [PubMed: 16585268]
13. Arimura N, Inagaki N, Chihara K, Menager C, Nakamura N, Amano M, et al. Phosphorylation of collapsin response mediator protein-2 by Rho-kinase. Evidence for two separate signaling pathways for growth cone collapse. The Journal of biological chemistry. 2000; 275:23973–80. [PubMed: 10818093]
14. Brown ME, Bridgman PC. Myosin function in nervous and sensory systems. Journal of neurobiology. 2004; 58:118–30. [PubMed: 14598375]
15. Hsieh SH, Ferraro GB, Fournier AE. Myelin-associated inhibitors regulate cofilin phosphorylation and neuronal inhibition through LIM kinase and Slingshot phosphatase. The Journal of neuroscience : the official journal of the Society for Neuroscience. 2006; 26:1006–15. [PubMed: 16421320]
16. Schwab ME, Strittmatter SM. Nogo limits neural plasticity and recovery from injury. Current opinion in neurobiology. 2014; 27:53–60. [PubMed: 24632308]
17. McKerracher L, Ferraro GB, Fournier AE. Rho signaling and axon regeneration. International review of neurobiology. 2012; 105:117–40. [PubMed: 23206598]
18. Bartus K, James ND, Bosch KD, Bradbury EJ. Chondroitin sulphate proteoglycans: key modulators of spinal cord and brain plasticity. Experimental neurology. 2012; 235:5–17. [PubMed: 21871887]
19. Raivich G. Transcribing the path to neurological recovery-From early signals through transcription factors to downstream effectors of successful regeneration. Ann Anat. 2011; 193:248–58. [PubMed: 21501955]
20. Yang P, Yang Z. Enhancing intrinsic growth capacity promotes adult CNS regeneration. Journal of the neurological sciences. 2012; 312:1–6. [PubMed: 21924742]
21. He Z, Jin Y. Intrinsic Control of Axon Regeneration. Neuron. 2016; 90:437–51. [PubMed: 27151637]
22. Shin JE, Cho YC, Beirowski B, Milbrandt J, Cavalli V, DiAntonio A. Dual Leucine Zipper Kinase Is Required for Retrograde Injury Signaling and Axonal Regeneration. Neuron. 2012; 74:1015–22. [PubMed: 22726832]
23. Grill, RJ., T, MH. Axonal responses to injury. CNS Regeneration: Academic Press; 1999.
24. Erturk A, Hellal F, Enes J, Bradke F. Disorganized microtubules underlie the formation of retraction bulbs and the failure of axonal regeneration. The Journal of neuroscience : the official journal of the Society for Neuroscience. 2007; 27:9169–80. [PubMed: 17715353]
25. Liu K, Lu Y, Lee JK, Samara R, Willenberg R, Sears-Kraxberger I, et al. PTEN deletion enhances the regenerative ability of adult corticospinal neurons. Nature neuroscience. 2010; 13:1075–81. [PubMed: 20694004]
26. Belin S, Nawabi H, Wang C, Tang S, Latremoliere A, Warren P, et al. Injury-induced decline of intrinsic regenerative ability revealed by quantitative proteomics. Neuron. 2015; 86:1000–14. [PubMed: 25937169]
27. Cai D, Qiu J, Cao Z, McAtee M, Bregman BS, Filbin MT. Neuronal cyclic AMP controls the developmental loss in ability of axons to regenerate. The Journal of neuroscience : the official journal of the Society for Neuroscience. 2001; 21:4731–9. [PubMed: 11425900]
28. Qiu J, Cafferty WB, McMahon SB, Thompson SW. Conditioning injury-induced spinal axon regeneration requires signal transducer and activator of transcription 3 activation. The Journal of neuroscience : the official journal of the Society for Neuroscience. 2005; 25:1645–53. [PubMed: 15716400]

29. Moore DL, Blackmore MG, Hu Y, Kaestner KH, Bixby JL, Lemmon VP, et al. KLF family members regulate intrinsic axon regeneration ability. Science. 2009; 326:298–301. [PubMed: 19815778]
30. Park KK, Liu K, Hu Y, Smith PD, Wang C, Cai B, et al. Promoting axon regeneration in the adult CNS by modulation of the PTEN/mTOR pathway. Science. 2008; 322:963–6. [PubMed: 18988856]
31. Sun F, Park KK, Belin S, Wang D, Lu T, Chen G, et al. Sustained axon regeneration induced by co-deletion of PTEN and SOCS3. Nature. 2011; 480:372–5. [PubMed: 22056987]
32. Geoffroy CG, Lorenzana AO, Kwan JP, Lin K, Ghassemi O, Ma A, et al. Effects of PTEN and Nogo Codeletion on Corticospinal Axon Sprouting and Regeneration in Mice. The Journal of neuroscience : the official journal of the Society for Neuroscience. 2015; 35:6413–28. [PubMed: 25904793]
33. Lu P, Yang H, Jones LL, Filbin MT, Tuszynski MH. Combinatorial therapy with neurotrophins and cAMP promotes axonal regeneration beyond sites of spinal cord injury. The Journal of neuroscience : the official journal of the Society for Neuroscience. 2004; 24:6402–9. [PubMed: 15254096]
34. Houle JD, Tom VJ, Mayes D, Wagoner G, Phillips N, Silver J. Combining an autologous peripheral nervous system “bridge” and matrix modification by chondroitinase allows robust, functional regeneration beyond a hemisection lesion of the adult rat spinal cord. The Journal of neuroscience : the official journal of the Society for Neuroscience. 2006; 26:7405–15. [PubMed: 16837588]
35. Wang X, Hasan O, Arzeno A, Benowitz LI, Cafferty WB, Strittmatter SM. Axonal regeneration induced by blockade of glial inhibitors coupled with activation of intrinsic neuronal growth pathways. Experimental neurology. 2012; 237:55–69. [PubMed: 22728374]
36. Lu P, Tuszynski MH. Growth factors and combinatorial therapies for CNS regeneration. Experimental neurology. 2008; 209:313–20. [PubMed: 17927983]
37. Benowitz LI, He Z, Goldberg JL. Reaching the brain: Advances in optic nerve regeneration. Experimental neurology. 2015
38. Siddiqui AM, Khazaei M, Fehlings MG. Translating mechanisms of neuroprotection, regeneration, and repair to treatment of spinal cord injury. Progress in brain research. 2015; 218:15–54. [PubMed: 25890131]
39. Gwak SJ, Nice J, Zhang J, Green B, Macks C, Bae S, et al. Cationic, amphiphilic copolymer micelles as nucleic acid carriers for enhanced transfection in rat spinal cord. Acta biomaterialia. 2016; 35:98–108. [PubMed: 26873365]
40. Livak KJ, Schmittgen TD. Analysis of relative gene expression data using real-time quantitative PCR and the 2(T)(-Delta Delta C) method. Methods. 2001; 25:402–8. [PubMed: 11846609]
41. Gwak SJ, Yun Y, Yoon do H, Kim KN, Ha Y. Therapeutic Use of 3beta-[N-(N′,N′-Dimethylaminoethane) Carbamoyl] Cholesterol-Modified PLGA Nanospheres as Gene Delivery Vehicles for Spinal Cord Injury. PloS one. 2016; 11:e0147389. [PubMed: 26824765]
42. Zukor K, Belin S, Wang C, Keelan N, Wang X, He Z. Short hairpin RNA against PTEN enhances regenerative growth of corticospinal tract axons after spinal cord injury. The Journal of neuroscience : the official journal of the Society for Neuroscience. 2013; 33:15350–61. [PubMed: 24068802]
43. Lewandowski G, Steward O. AAVshRNA-mediated suppression of PTEN in adult rats in combination with salmon fibrin administration enables regenerative growth of corticospinal axons and enhances recovery of voluntary motor function after cervical spinal cord injury. The Journal of neuroscience : the official journal of the Society for Neuroscience. 2014; 34:9951–62. [PubMed: 25057197]
44. Zhou HX, Li XY, Li FY, Liu C, Liang ZP, Liu S, et al. Targeting RPTPsigma with lentiviral shRNA promotes neurites outgrowth of cortical neurons and improves functional recovery in a rat spinal cord contusion model. Brain research. 2014; 1586:46–63. [PubMed: 25152470]
45. Wu HF, Cen JS, Zhong Q, Chen L, Wang J, Deng DY, et al. The promotion of functional recovery and nerve regeneration after spinal cord injury by lentiviral vectors encoding Lingo-1 shRNA delivered by Pluronic F-127. Biomaterials. 2013; 34:1686–700. [PubMed: 23211450]

46. Campos SK, Barry MA. Current advances and future challenges in Adenoviral vector biology and targeting. Current gene therapy. 2007; 7:189–204. [PubMed: 17584037]
47. Kay MA, Glorioso JC, Naldini L. Viral vectors for gene therapy: the art of turning infectious agents into vehicles of therapeutics. Nat Med. 2001; 7:33–40. [PubMed: 11135613]
48. Yin H, Kanasty RL, Eltoukhy AA, Vegas AJ, Dorkin JR, Anderson DG. Non-viral vectors for gene-based therapy. Nature Reviews Genetics. 2014; 15:541–55.
49. Mintzer MA, Simanek EE. Nonviral Vectors for Gene Delivery. Chem Rev. 2009; 109:259–302. [PubMed: 19053809]
50. Cutlar L, Zhou D, Hu X, Duarte B, Greiser U, Larcher F, et al. A non-viral gene therapy for treatment of recessive dystrophic epidermolysis bullosa. Experimental dermatology. 2016; 25:818–20. [PubMed: 27117059]
51. Otsuka S, Adamson C, Sankar V, Gibbs KM, Kane-Goldsmith N, Ayer J, et al. Delayed intrathecal delivery of RhoA siRNA to the contused spinal cord inhibits allodynia, preserves white matter, and increases serotonergic fiber growth. Journal of neurotrauma. 2011; 28:1063–76. [PubMed: 21443453]
52. Cheng X, Fu R, Gao M, Liu S, Li YQ, Song FH, et al. Intrathecal application of short interfering RNA knocks down c-jun expression and augments spinal motoneuron death after root avulsion in adult rats. Neuroscience. 2013; 241:268–79. [PubMed: 23506737]
53. Wu Y, Yang L, Mei X, Yu Y. Selective inhibition of STAT1 reduces spinal cord injury in mice. Neurosci Lett. 2014; 580:7–11. [PubMed: 24321405]
54. Rejman J, Oberle V, Zuhorn IS, Hoekstra D. Size-dependent internalization of particles via the pathways of clathrin- and caveolae-mediated endocytosis. The Biochemical journal. 2004; 377:159–69. [PubMed: 14505488]
55. Hayakawa K, Uchida S, Ogata T, Tanaka S, Kataoka K, Itaka K. Intrathecal injection of a therapeutic gene-containing polyplex to treat spinal cord injury. Journal of controlled release : official journal of the Controlled Release Society. 2015; 197:1–9. [PubMed: 25449800]
56. Sung JK, Miao L, Calvert JW, Huang L, Louis Harkey H, Zhang JH. A possible role of RhoA/Rho-kinase in experimental spinal cord injury in rat. Brain research. 2003; 959:29–38. [PubMed: 12480155]
57. Dubreuil CI, Winton MJ, McKerracher L. Rho activation patterns after spinal cord injury and the role of activated Rho in apoptosis in the central nervous system. The Journal of cell biology. 2003; 162:233–43. [PubMed: 12860969]
58. Madura T, Yamashita T, Kubo T, Fujitani M, Hosokawa K, Tohyama M. Activation of Rho in the injured axons following spinal cord injury. EMBO reports. 2004; 5:412–7. [PubMed: 15031718]
59. Li Z, Dong X, Wang Z, Liu W, Deng N, Ding Y, et al. Regulation of PTEN by Rho small GTPases. Nature cell biology. 2005; 7:399–404. [PubMed: 15793569]
60. Lai TW, Zhang S, Wang YT. Excitotoxicity and stroke: identifying novel targets for neuroprotection. Progress in neurobiology. 2014; 115:157–88. [PubMed: 24361499]
61. Bertrand J, Winton MJ, Rodriguez-Hernandez N, Campenot RB, McKerracher L. Application of Rho antagonist to neuronal cell bodies promotes neurite growth in compartmented cultures and regeneration of retinal ganglion cell axons in the optic nerve of adult rats. J Neurosci. 2005; 25:1113–21. [PubMed: 15689547]
62. Impellizzeri D, Mazzon E, Paterniti I, Esposito E, Cuzzocrea S. Effect of fasudil, a selective inhibitor of Rho kinase activity, in the secondary injury associated with the experimental model of spinal cord trauma. The Journal of pharmacology and experimental therapeutics. 2012; 343:21–33. [PubMed: 22733360]
63. Bertrand J, Di Polo A, McKerracher L. Enhanced survival and regeneration of axotomized retinal neurons by repeated delivery of cell-permeable C3-like Rho antagonists. Neurobiology of disease. 2007; 25:65–72. [PubMed: 17011202]

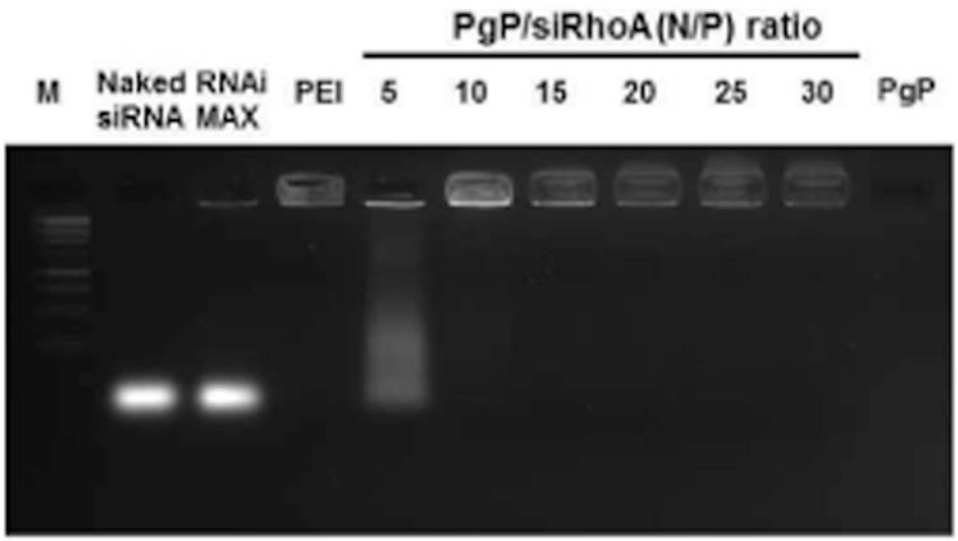

Figure 1.

Gel retardation assay of PgP/siRhoA polyplexes prepared at varying N/P ratios electrophoresed on 2 % agarose gel: 1 kb DNA molecular weight marker (Lane 1), naked siRhoA (lane 2), RNAiMAX/siRhoA (lane 3), bPEI/siRhoA at N/P ratio of 5/1 (lane 4), PgP/siRhoA prepared at N/P ratios of 5/1, 10/1, 15/1, 20/1, 25/1, and 30/1 (lane 5, 6, 7, 8, 9, and 10), and PgP alone (lane 11).

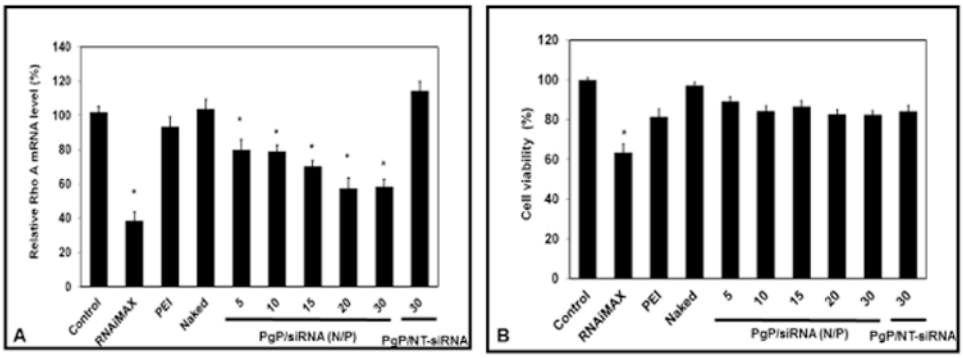

Figure 2.

RhoA knockdown efficiency (A) and cell viability (B) after transfection of PgP/siRhoA polyplexes prepared at varying N/P ratios in neuroblastoma (B35) cells in media containing 10 % serum. At 72 hours post-transfection, RhoA expression level was determined by RT-PCR and cell viability was determined by MTT assay. Data represent the mean ± SEM (n=6). *: $P<0.05$ compared to untreated control.

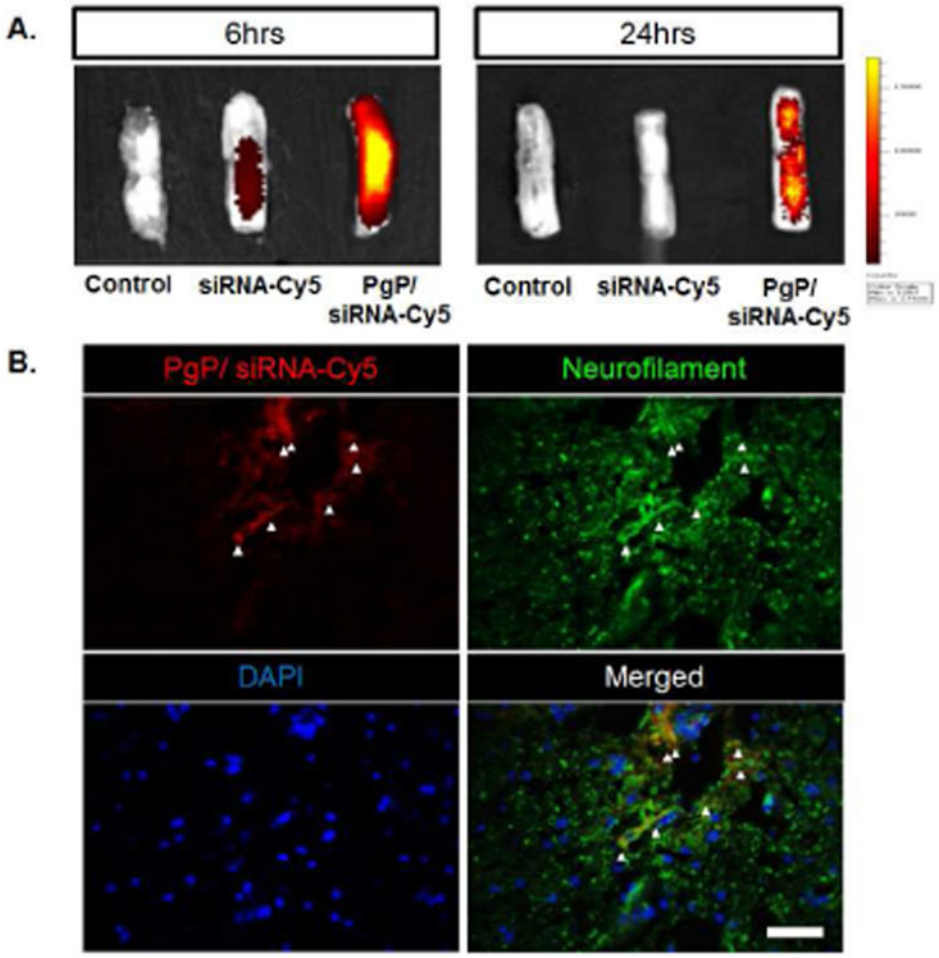

Figure 3.

Retention and cellular uptake of PgP/siRNA-Cy5 polyplexes (N/P ratio of 30/1, 10 μg siRNA-Cy5) after local injection in SCI lesion site. (A) *Ex vivo* fluorescent imaging of PgP/siRNA-Cy5 in spinal cord injury at 6 and 24 hours post-injection. (B) Visualization of PgP/siRNA-Cy5 polyplex uptake by neuronal cells in spinal cord lesion site at 24 hours post-injection. PgP/siRNA-Cy5 polyplex (Red), immunofluorescent staining for neurofilament (NF, Green), and DAPI counterstained nuclei (blue). Scale bar indicates 50 μm.

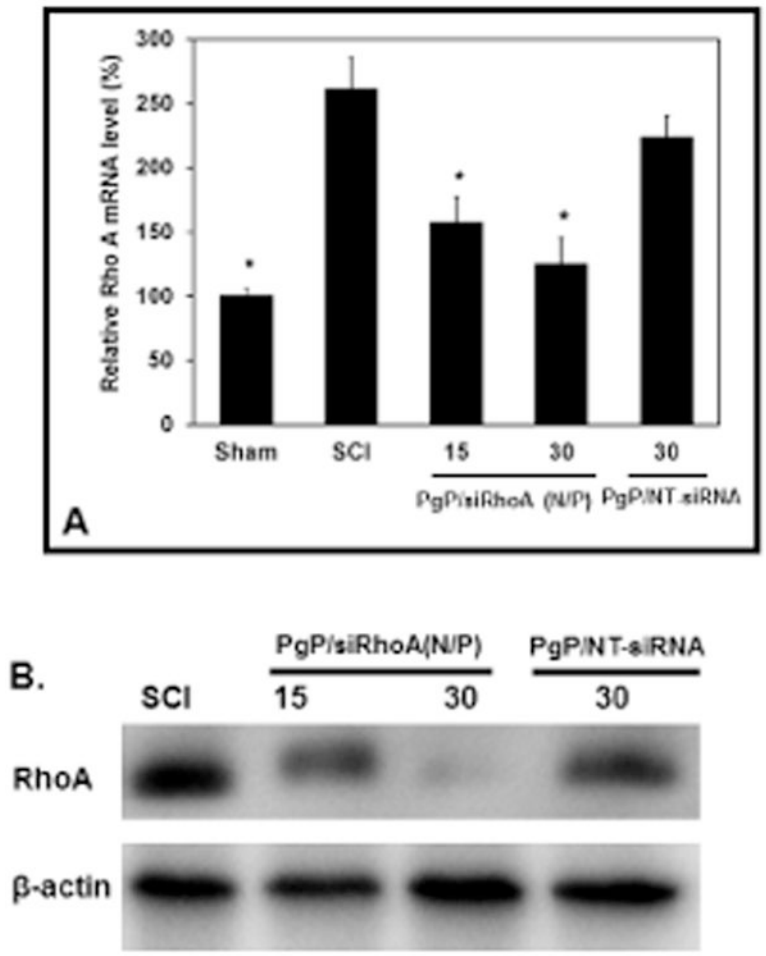

Figure 4.

Rho A knockdown efficiency of PgP/siRhoA polyplexes (two N/P ratios: 15/1 and 30/1, siRhoA : 10 μg siRhoA) after local injection in SCI lesion site. At 7 days post-injury, animals were sacrificed and spinal cord (0.5 cm-long piece from the center of the injury) was harvested for RT-PCR and western blot. Control: Sham animal group, SCI: untreated SCI animal group, 15/1: PgP/siRhoA polyplexes at N/P ratio of 15/1, 30/1: PgP/siRhoA polyplexes at N/P ratio of 30/1, and PgP/NT-siRNA 30/1: PgP/non-targeting-siRNA polyplexes at N/P ratio of 30/1, (A) Relative RhoA mRNA level by real-time qRT-PCR. Glyceraldehyde-3-phosphate dehydrogenase (GAPDH) was used as an endogenous control. *: $P<0.05$ compared to untreated SCI group, (B) RhoA protein level by western blot. β-actin was used as endogenous control.

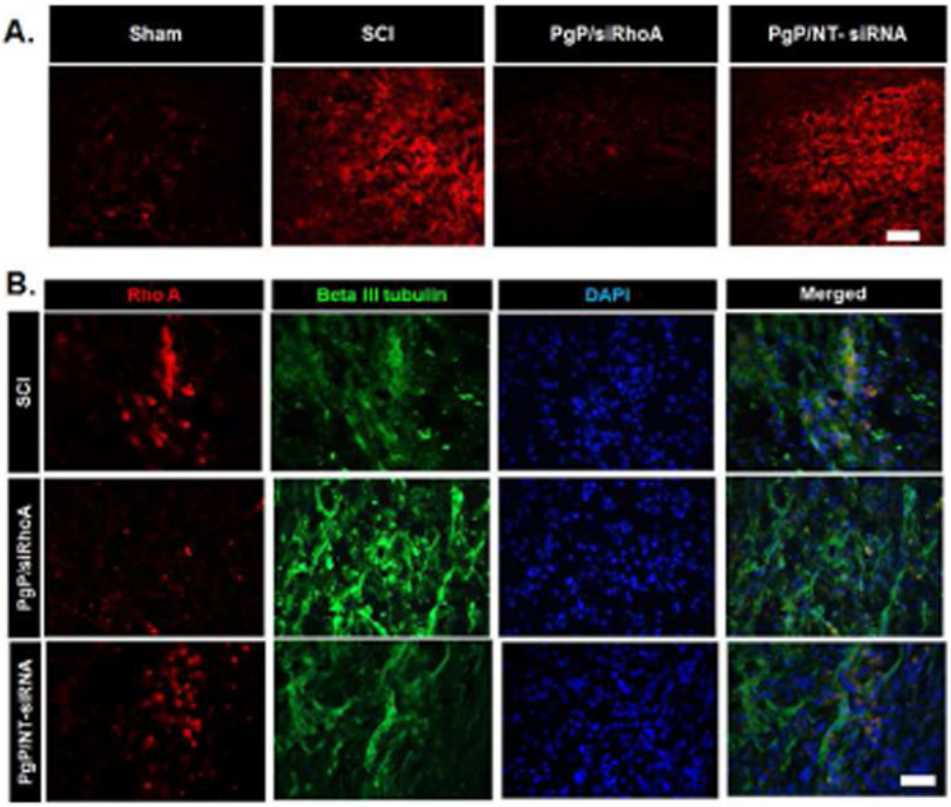

Figure 5.

Immunohistochemical staining for RhoA after local injection of PgP/siRhoA polyplexes (N/P ratio of 30/1, siRhoA: 10 μg). At 1 week post-injury, spinal cords were harvested and sectioned longitudinally. Untreated SCI and PgP/NT-siRNA polyplexes (N/P ratio 30/1, NT-siRNA: 10 μg) were used for comparison. (A) IHC staining for RhoA (red), scale bar: 200 μm. (B) Double-IHC staining for RhoA (red), neuron-specific β-III Tubulin (green) and DAPI (blue). Scale bar indicates 50 μm.

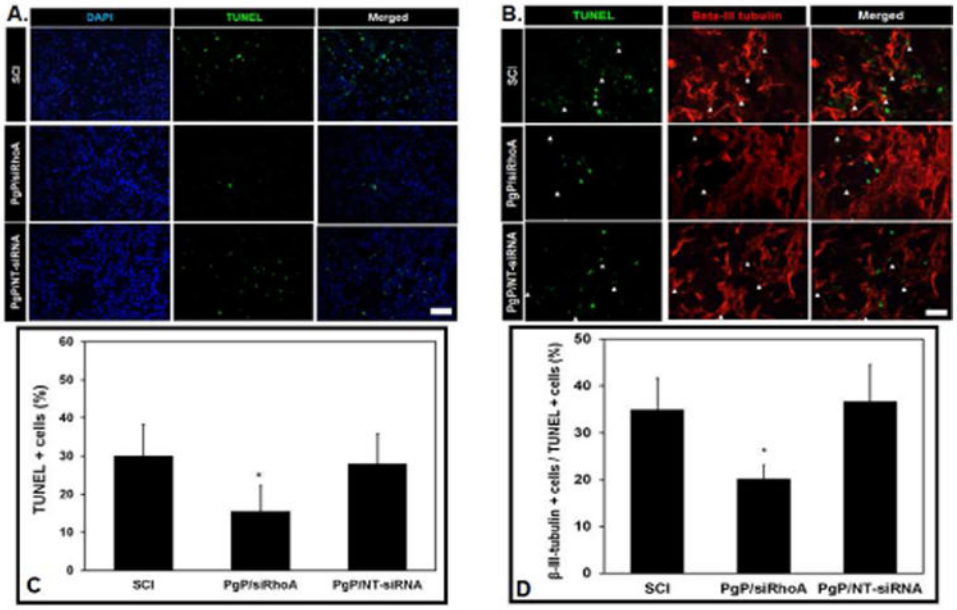

Figure 6.

Effect of RhoA knockdown by PgP/siRhoA polyplexes (N/P ratio 30/1, siRhoA : 10 μg) on apoptosis by TUNEL assay. At 7 days post-injury, the spinal cords were harvested and sectioned longitudinally and stained by the ApopTag Plus Fluorescein In situ Apoptosis Detection kit. Untreated SCI and PgP/NT-siRNA polyplexes (N/P ratio 30/1, NT-siRNA: 10 μg) were used for comparison. (A) Cell nuclei (DAPI, blue) and TUNEL+ cells (green). Scale bar: 100 μm. (B) Double IHC staining for TUNEL+ (green) and beta III tubulin+ (red) cells. Scale bar: 50 μm. (C) The % TUNEL-positive cells in untreated SCI and after injection of PgP/siRhoA or PgP/NT-siRNA polyplexes was quantified from total 15 different sections of spinal cords from each group (3 sections/rat, 5 rats/group). $*p < 0.05$ compared with untreated SCI. (D) The % beta-III tubulin+ cells in total TUNEL+ cells in spinal cord lesion site was quantified from total 15 different sections of spinal cords from each group (3 sections/rat, 5 rats/group). $*p < 0.05$ compared with untreated SCI.

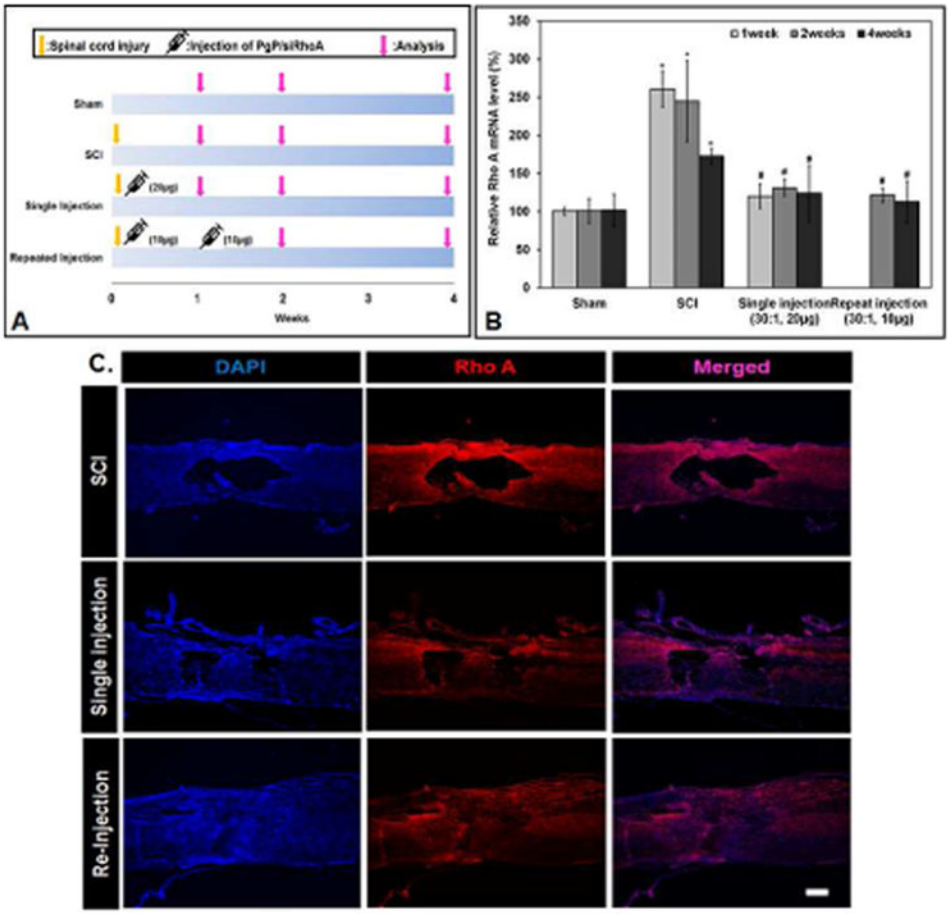

Figure 7.

(A) Experimental design for PgP/siRhoA administration timing and outcome assessment over a 4 week time period. Single injection: PgP/siRhoA polyplexes (N/P 30/1, siRhoA 20 μg) were locally injected in the lesion site immediately after SCI injury. Repeat injection: PgP/siRhoA polyplex (N/P 30/1, siRhoA 10 μg/injection) was locally injected in the lesion site immediately after SCI injury and at 1 week post-injury. At 1, 2, and 4 weeks post-injury, spinal cords (0.5 cm-long piece from the center of the injury) were harvested and RhoA knockdown was evaluated by RT-PCR and IHC. (B) RhoA mRNA expression levels evaluated by RT-PCR. Sham animal group and untreated SCI group were used as controls (n=5/group). GAPDH was used as an endogenous control. *P<0.05 compared to Sham, # P<0.05 compared to SCI. (C) Longitudinal sections of SCI lesion sites stained for RhoA (red) and cell nuclei (blue, DAPI) at 4 weeks post-injury. Untreated SCI (top), single-injection (middle), and re-injection (bottom).

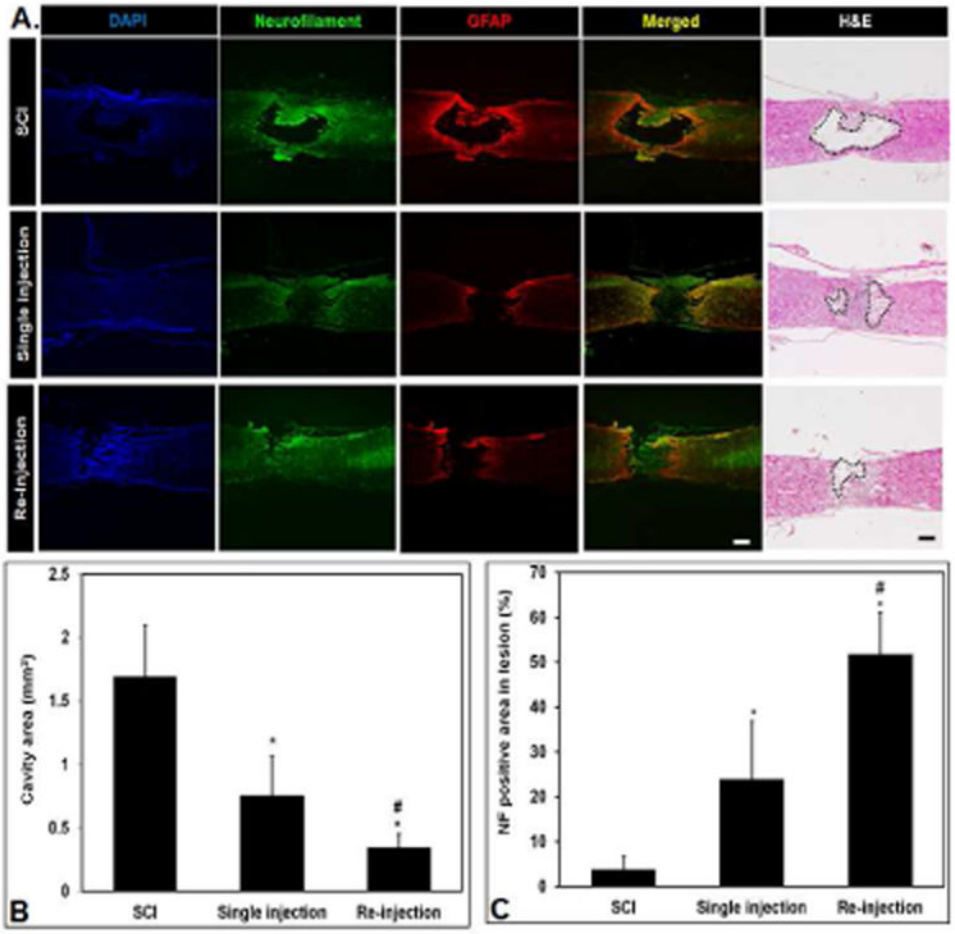

Figure 8.

Immunohistological assessment of lesion sites 4 weeks after SCI and injection of PgP/siRhoA polyplexes. (A) Representative images of immunostaining for neurofilament (green), GFAP (red), and DAPI (blue) and hematoxylin and eosin staining to measure cavity area. Scale bars: 400 μm. Untreated SCI (top) shows an extensive necrotic lesion cavity and significant reactive astrogliosis, Single-injection (middle) and re-injection (bottom) animal group shows reduced cavitation/astrogliosis and axonal regeneration in the lesion site. (B) Quantification of necrotic cavity area (mm^2) in the lesion of spinal cord at 4 weeks post-injection of PgP/siRhoA polyplexes. The cavity area was measured from total 15 different sections of spinal cord from each group (3 sections/rat, 5 rats/each group) after hematoxylin and eosin staining. *$P<0.05$ compared to untreated SCI, $^{\#}P<0.05$ compared to single injection of PgP/siRhoA polyplexes. (C) Quantification of neurofilament (NF) positive (+) axons in the lesion site. The NF positive area in the lesion site was measured from total 15 different sections of spinal cord from each group (3 sections/rat, 5 rats/each group). The % NF positive area was calculated as a percentage of the total necrotic cavity area measured from hematoxylin and eosin staining. *$P<0.05$ compared to untreated SCI, $^{\#}P<0.05$ compared to single injection of PgP/siRhoA polyplexes.